Developments in the Built Environment 17 (2024) 100366

Contents lists available at ScienceDirect

Developments in the Built Environment

journal homepage: www.sciencedirect.com/journal/developments-in-the-built-environment

Uncertainty effect on seismic capacity assessment in the out-of-plane failure mechanisms of masonry structures by probabilistic and non-probabilistic approaches

Matteo Mazzeo, Rossella Laudani, Roberta Santoro *

Dipartimento di Ingegneria, Università degli Studi di Messina, C. da Di Dio, 98166, Messina, Italy

ARTICLE INFO

Keywords:
Masonry
Out-of-plane failure mechanisms
Seismic acceleration capacity
Uncertainty quantification
Stochastic analysis
Uncertain-but-bounded variables

ABSTRACT

The present paper aims to provide a contribution in the study of the seismic analysis of existing masonry structures in presence of uncertain parameters described by following both probabilistic and non-probabilistic models. By posing the attention on the local out-of-plane failure mechanisms, the non-deterministic analysis is conducted on the kinematic chains of masonry portions by first applying the upper bound theorem of the limit analysis providing the expressions of the load multiplier parameter and in turn the acceleration capacity of the local mechanism with an explicit dependence on the uncertainties. Specifically, two particular local failure mechanisms commonly observed in post-earthquake scenarios, namely the vertical bending mechanism and the corner overturning mechanism, are analyzed considering the masonry-specific weight, the position of the cylindrical hinge and the cracks lines inclination as uncertain variables. In the framework of a stochastic approach, the uncertain parameters are described by random variables with assigned probability density functions (PDFs) and the Probability Transformation Method is applied to return the PDFs of the seismic response functions. In a non-probabilistic setting, the same parameters are defined as uncertain-but-bounded variables in terms of lower and upper bounds and a global optimization technique straightforwardly allows to estimate the intervals for the seismic response functions. Taking full advantage of the close link between the two proposed approaches, the numerical investigations allow to better understand whether the interval analysis is adequate for a reliable assessment of the seismic acceleration capacity or a stochastic analysis is preferable and therefore a more in-depth experimental campaign is required to fully describe the uncertain input parameters as random variables. Moreover, results on the separate and combined effect of the uncertain parameters on the seismic response functions provide other useful information to predict the masonry capacity and preserve integrity.

1. Introduction

Unreinforced masonry buildings represent the majority of cultural heritage. Due to the different types of units and mortar used in the construction together with several number of their possible combinations, the existing masonry structures show a remarkable variety of configurations which in turn influence their structural behaviors. Regardless of the masonry properties and the construction technique, a common feature of the existing masonry buildings consists in the high vulnerability to seismic actions as revealed by the catastrophic seismic events that occurred in the past and especially in recent years (e.g. earthquakes of L'Aquila, 2009; Emilia Romagna, 2012; and Central Italy, 2016 in the Italian country). In this regard, the seismic analysis of historic masonry structures has attracted considerable attention; most of the present studies (Mendes and Lourenço, 2014; de Felice et al., 2017; Chácara et al., 2016, 2018; Zhang et al., 2022) are devoted to the prediction of their capacity in order to preserve structural integrity and ensure the safety. In general, the high sensitivity of masonry structures to horizontal seismic loads involves the activation of damage mechanisms that can be grouped into two classes: in-plane and out-of-plane damage mechanisms. All the in-plane failure mechanisms are usually labeled as "global mechanisms" because they can occur when the whole building presents the so-called box-behavior generally guaranteed by a good connection between walls as well as between walls and roof and in the presence of rigid horizontal diaphragms. They are governed by the in-plane lateral capacity of walls and pier-spandrel systems which offers

* Corresponding author.
E-mail address: roberta.santoro@unime.it (R. Santoro).

https://doi.org/10.1016/j.dibe.2024.100366
Received 3 November 2023; Received in revised form 3 February 2024; Accepted 10 February 2024
Available online 14 February 2024

better performance against seismic action. Otherwise, the existing ancient masonry buildings due to their general conditions often characterized by low construction quality, absence of proper connections between structural components and insufficient stiffness of horizontal floors could be affected by the loss of stability of parts of the structure exhibiting out-of-plane failure mechanisms (Lourenço et al., 2011; Valluzzi et al., 2014; Giresini et al., 2019, 2021; Casapulla et al., 2021).

The latter ones consist in local responses of the walls, typically depending on both the poor connections among the orthogonal walls and structural elements as well as their quality and slenderness, thus inhibiting a box-type global response of the structure and often involving partial or total collapses of walls. Under seismic actions and favored by previous cracking patterns, the local out-of-plane failure mechanisms are the first to activate and undoubtedly the most dangerous among all the possible failures of unreinforced masonry structures under horizontal loading and will be the object of the present study. The analysis for the out-of-plane failure mechanisms is therefore conducted on kinematic chains of masonry portions, regarded as rigid macroblock assemblages, interacting through interface elements. One of the most common approaches to assess the masonry structure capacity is based on the upper bound theorem of the limit analysis (Heyman, 1966) which allows the estimation of the so-called "load multiplier" parameter responsible of the local failure mechanism (Italian Building code (Decreto 17 gennaio 2018, 2018) generally defined by the acronym NTC2018) and in turn the acceleration capacity. Multiple (theoretically infinite) failure mechanisms need to be considered to estimate the minimum of the kinematically compatible load multipliers. The load multiplier evaluation highly depends on the macroblocks' geometry considered in the out-of-plane failure mechanisms models. In this regard, a more realistic prediction of the out-of-plane failure mechanisms and a reliable estimate of the seismic acceleration capacity are required to account for the uncertainties in the models of the kinematic chain involving macroblocks. As stated previously, the uncertain parameters to consider are mainly linked to the shape of the macroblock in terms of weight, geometry and position of the cylindrical hinge where the rotation of the block itself is assumed.

Recently some studies have incorporated the uncertainties in the assessment of masonry structures and in the seismic capacity estimation: in all these analyses the parameters describing the masonry material properties have been treated as random variables to take into account the several factors influencing their exact assignment.

In (Parisi and Augenti, 2012) based on a preliminary statistical characterization of mechanical parameters of existing masonry types, realizations of a random modeling vector were implemented in a macroelement capacity model of the structure and static push-over analysis was performed for each code-based load combination and lateral load pattern to assess the seismic capacity of an entire two-story unreinforced masonry building. In (Pulatsu et al., 2022) a probabilistic computational modeling framework using the discrete element method has been proposed to predict structural behavior and capacity of load-bearing unreinforced masonry systems considering uncertainties in material properties by performing Monte Carlo simulations to yield various failure modes related to shear cracks in the piers, flexural and/or shear cracking of the spandrel or their combinations. In the framework of finite element modeling strategy developed for unreinforced masonry walls subjected to in-plane lateral loading, the influence of spatial variability of material properties within these unreinforced masonry walls was examined through the application of Monte Carlo simulations (Gooch et al., 2021).

In (Saloustros et al., 2019) the seismic vulnerability of historical masonry structures considering uncertainty in the material parameters has been assessed via a probabilistic approach based on the Monte Carlo simulation; the aim of the stochastic analysis, which considers the pushover analysis using the finite element method for the structural evaluation of the seismic behavior of masonry structures, is to investigate the effect of the uncertainty of the structural members' mechanical parameters on the evaluation of the seismic fragility. In (Tomić et al., 2021) Latin Hypercube Sampling (LHS) was performed to account for the epistemic uncertainty of material and modeling parameters with applications on a stiff monumental historical masonry building and a tall and slender residential masonry building.

All the above-cited studies demonstrated the importance of stochastic modeling on capacity and behavior prediction and highlighted the need for substantial research to quantify the uncertainties in the analysis; nevertheless, they are limited to global analyses and in-plane damage mechanisms, focusing attention in almost all cases on the uncertainties relating to the properties of the material using Monte Carlo simulation in a probabilistic approach framework. The present study focuses on how the introduction of uncertain parameters in the modeling of local out-of-plane mechanisms could affect the assessment of seismic capacity. To address this issue, firstly two perspectives are considered in the description of uncertain variable parameters. In a probabilistic framework, under the assumption of possessing sufficient experimental data, the uncertain parameters affecting the material unit weight and the geometry of the macroblocks are described by random variables with assigned probability density functions (PDFs) and therefore a probabilistic method can be handled for the stochastic analysis. Whereas in a non-probabilistic context, the same parameters are defined as interval variables (also labeled as uncertain-but-bounded variables) in terms of lower and upper bounds or alternatively defined in terms of a central (or midpoint) value and a deviation. The interval model (based mainly on the interval arithmetic introduced by Moore (Moore and Yang, 1996)) turns out to be the most useful analytical tool to handle uncertain parameters described by fragmentary or incomplete data, which is, furthermore, a very frequent condition when dealing with existing masonry structures. Thus, taking full advantage of the analytical forms provided by the application of limit analysis for the load multiplier as well as for the acceleration capacity with an explicit dependence on the uncertain parameters, two different procedures are applied. Specifically, the Probability Transformation Method (PTM) (Laudani and Falsone, 2021; Falsone and Laudani, 2020), employed in the stochastic setting, returns the PDFs of both the load multiplier and in turn the acceleration; within a non-probabilistic framework, a global optimization technique (Elishakoff and Ohsaki, 2010; Santoro et al., 2015, 2020; Santoro and Failla, 2021) allows to evaluate their bounds. The estimated intervals are directly compared with the response PDFs, providing a confirmation of the main results previously obtained by the authors in (Laudani and Santoro, 2022) and allowing a deeper insight into the choice of uncertain parameters modeling in non-deterministic analysis. The numerical studies are conducted on two specific collapse mechanisms quite widespread in post-earthquake scenarios, namely the vertical bending mechanism and the corner overturning mechanism. In particular, the corner overturning failure is investigated for a damaged real building after the 2016–2017 Central Italy earthquake sequence. The results in terms of dispersion in load multiplier as well as in terms of spectral acceleration capacity can guide the decision-making in design solutions depending in turn on seismic capacity predictions.

2. Out-of-plane local failure mechanisms

The existing masonry structures often manifest local failure mechanisms; their formation depends on several factors such as the geometry of the masonry walls, the masonry mechanical properties, the quality of the connections between walls, and between walls and floors/roof, the boundary conditions, the diaphragms flexibility, and the entity of static loads as well as the seismic input acting on the building.

As previously outlined, the limit analysis based on the upper bound theorem (Heyman, 1966) is a classic approach used in structural engineering to estimate the load multiplier responsible for the activation of the local mechanism: it relies on a simplified model of the masonry behavior which is considered as a rigid material with infinite compressive strength and zero tensile strength. The analysis is carried out

following a linear kinematic approach involving masonry walls (or parts of facades), treated as rigid bodies without sliding between blocks.

The simplified model adopted in the limit analysis has the advantage of being independent of the masonry material properties; however, the results of the analyses are strongly influenced by the geometry of the macro-blocks and by the proper identification of the corresponding failure surfaces. Once each possible local mechanism is identified in the investigated structure, the corresponding load multiplier α associated with its activation must be evaluated: in a real case scenario, the local mechanism most likely to be triggered is the one associated with the lowest value of the identified load multipliers, herein labeled as α_0.

In the following two subsections, the vertical bending mechanism and the corner overturning mechanism are analyzed in detail via limit analysis. In both cases, the formulations are conducted by recalling the basic steps of linear kinematic analysis considering all involved parameters at their deterministic values.

2.1. Vertical bending mechanism

The vertical bending mechanism typically develops when masonry walls are bounded at top and bottom but no connection is present in the center part; the typical situation is represented by a masonry building with an RC curb on top and poorly connected at the intermediate floors. Fig. 1 illustrates the geometric scheme of the investigated mechanism: W_i (with $i = 1, 2$) represents the weight of the i-th block involved in the mechanism, h and s are the height and thickness of the wall, respectively, whereas h_i (with $i = 1, 2$) represents the height of the i-th block. In particular, to correlate the height of each block to the total height of the wall, a parameter μ can be introduced, such as the following expressions can be derived:

$$h_1 = \frac{\mu - 1}{\mu} h; \quad h_2 = \frac{h}{\mu} \quad \text{with} \quad \mu > 0 \tag{1}$$

Further, the most common load conditions are considered in the investigation, namely the load contribution N related to permanent and variable load due to the overlying structural elements, the vertical load P due to the intermediate floor and the corresponding horizontal static thrust S which are applied as shown in Fig. 1.

When this mechanism is triggered the crack pattern usually presents a horizontal failure surface along the facade modeled by a horizontal cylindrical hinge dividing the wall into two blocks that can rotate around the hinge axis of an angle θ and ψ, respectively (see Fig. 1). The load multiplier α is thus obtained by applying the Principle of Virtual Work (PVW), in terms of displacements reported in Table 1, by equating the total work performed by external forces, applied to the system in correspondence with a virtual motion, to the work of any internal forces of the system.

It is worth noting that, the expression of the PVW varies in function of the position of the point of application h_s of the horizontal loads (see Fig. 1(a) and (b)). In particular, it is possible to derive two different expressions where in the first case the horizontal load's application point is above the hinge representative of the damaged surface (see Fig. 1(a)) while in the second case, it is below the hinge (see Fig. 1(b)). It follows that the virtual displacements $\delta_{y,P}$ and $\delta_{x,S}$ assume, respectively, the two expressions reported in Table 1.

In detail:

- Case 1: the position of the hinge defined by h_1 is below h_s value (see Fig. 1(a)). In this case, the load of the intermediate floor, P, and the corresponding thrust S are applied to block 2. Therefore, it is possible to write:

$$\alpha\left(W_1\delta_{x,W_1} + W_2\delta_{x,W_2} + P((h-h_s)\psi)\right) - W_1\delta_{y,W_1} - W2\delta_{y,W_2} - N\delta_{y,N} - P\delta(s\theta + e\psi) + S((h-h_s)\psi) = 0 \tag{2}$$

then, the expression labeled as α_{case_1} takes the following form:

Table 1
Vertical bending mechanism: virtual displacements adopted in the PVW.

Virtual displacements - vertical bending mechanism
$\delta_{x,W_1} = \frac{h_1}{2}\theta = \frac{(\mu-1)h}{2\mu}\theta$
$\delta_{y,W_1} = \frac{s}{2}\theta$
$\delta_{x,W_2} = \frac{h_2}{2}\psi = \frac{(\mu-1)h}{2\mu}\theta$
$\delta_{y,W_2} = s\theta + \psi\frac{s}{2} = \frac{(\mu+1)s}{2}\theta$
$\delta_{y,N} = s\theta + d\psi = [s + d(\mu-1)]\theta$
$\delta_{y,P} = s\theta + e\psi = [s + e(\mu-1)]\theta$ (case 1) $\vee$ $\delta_{y,P} = (s-e)\theta$ (case 2)
$\delta_{x,S} = (h-h_s)\psi = (h-h_s)(\mu-1)\theta$ (case 1) $\vee$ $\delta_{x,S} = h_s\theta$ (case 2)

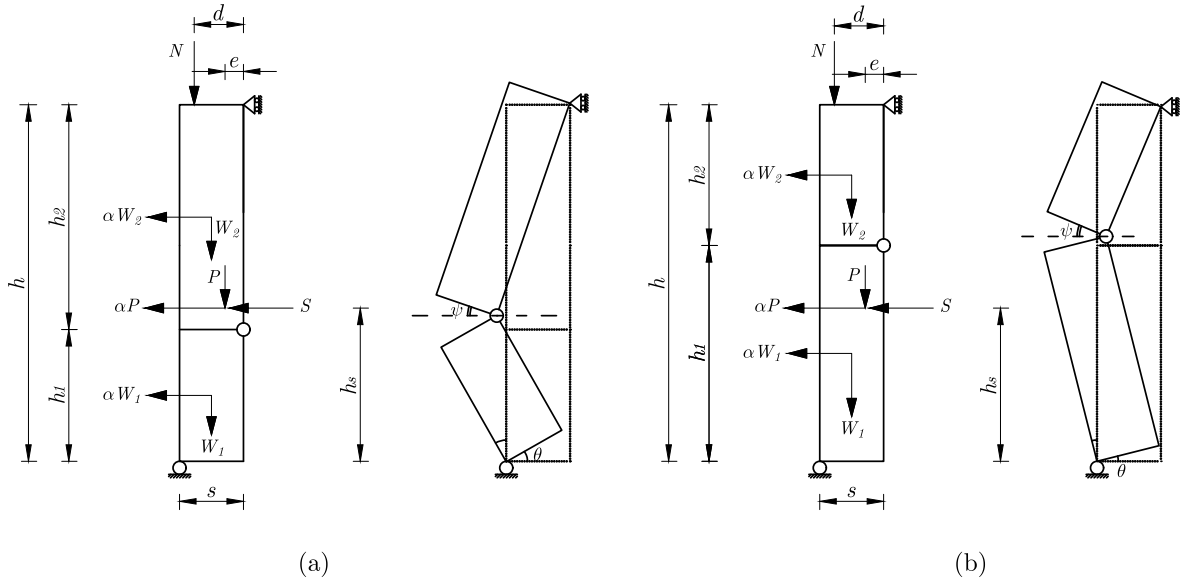

Fig. 1. Vertical bending mechanism depending on the position of the hinge: (a) $h_1 < h_s$ and (b) $h_1 > h_s$.

$$\alpha_{\text{case}_1} = \frac{2\mu((N+P+W_1+W_2)s+Nd(\mu-1)+Pe(\mu-1)-S(h-h_s)(\mu-1))}{(\mu-1)((W_1+W_2)h+2P\mu(h-h_s))} \tag{3}$$

· Case 2: the position of the hinge is above the h_s value (see Fig. 1(b)). In this case, the load of the intermediate floor, P, and the thrust S are applied to block 1. Therefore, the PVW reads:

$$\alpha\left(W_1\delta_{x,W_1}+W_2\delta_{x,W_2}+Ph_s\theta\right)-W_1\delta_{y,W_1}-W_2\delta_{y,W_2}-N\delta_{y,N}-P(s-e)\theta + S_{tot}h_s\theta = 0 \tag{4}$$

then, the expression of α, labeled as α_{case_2}, can be derived as:

$$\alpha_{\text{case}_2} = \frac{2\mu(-Pe-Sh_s+(N+P+W_1+W_2)s+Nd(\mu-1))}{(W_1+W_2)(\mu-1)h+2P\mu h_s} \tag{5}$$

In both Eqs. (3) and (5), the weights W_1 and W_2 of the macroblocks explicitly depend on both the hinge position μ and the masonry specific weight γ as follows:

$$W_1 = \gamma sLh\frac{\mu-1}{\mu}; \quad W_2 = \frac{\gamma sLh}{\mu} \tag{6}$$

where s is the thickness of the masonry wall and L is its length. In this deterministic framework, the minimum load multiplier α_0, responsible for the local mechanism activation, can be obtained as the global minimum of the piece-wise function made up of Eqs. (3) and (5) defined in different domains depending on the specific range of values assumed by the normalized hinge height μ.

2.2. Corner overturning mechanism

In this subsection, the corner overturning mechanism, typical of a structure with a hip roof is investigated. As can be seen from Fig. 2, this mechanism occurs through the rigid rotation of a detached wedge which is delimited by diagonal fracture surfaces in perpendicular walls.

Under the assumption that no window openings are present in the proximity to the corner and that the masonry walls have the same material and thickness s on both sides, the overturning mechanism will be characterized by crack lines with the same inclination θ with respect to the vertical line, i.e. C_1=C_2=C. Specifically, the corner overturning will take place around an axis passing through point A (see Fig. 2), orthogonal to the corner bisector plane of the wedge. The load analysis conducted for the mechanism includes the weight of the involved masonry blocks W_i, the localized vertical load P_{v0} produced by the hip rafter on the corner, the corresponding horizontal static thrust P_{h0}, the vertical load $P_{vi} = q_iC_i$ (with $i = 1, 2$) acting on the i-th wall and the corresponding static thrust P_{hi}. For the mechanism represented in Fig. 2, the application of the PVW providing the load multiplier α is equivalent to equaling the stabilizing and overturning moment expressions, M_s and M_o respectively.

Specifically, the stabilizing moment can be evaluated as follows:

$$M_s = \sum_i W_i d_{w_i} + P_{v_0}d_{P_{v_0}} + P_{v_1}d_{P_{v_1}} + P_{v_2}d_{P_{v_2}} \tag{7}$$

while the overturning moment expression reads:

$$M_o = \alpha\left(W_0\frac{h}{2}+W_1\frac{2h}{2}+W_2\frac{2h}{3}+(P_{v_0}+P_{v_1}+P_{v_2})h\right)+\left(P_{h_0}+P'_{h_1}+P'_{h_2}\right)h \tag{8}$$

where h is the height of the masonry corner involved in the mechanism whereas the superscript refers to the projection of the forces in the direction of the overturning, i.e. $\beta = 45°$, obtained by multiplying their values by $\sqrt{2}/2$. The weights of the masonry corner elements, namely W_i ($i = 0, 1, 2$), are explicitly dependent on the hinge position μ (for uniformity of notation with the previous case it is considered that $\mu = h_s$), on the specific weight γ and on the crack lines inclination θ as follows:

$$W_0 = \gamma s^2(H-\mu); \quad W_1 = W_2 = \frac{\gamma(H-\mu)^2\tan(\theta)}{2} \tag{9}$$

It is worth noticing that also the lever arms d_j ($j = W_i, P_{v_i}, P_{h_i}$) of each vertical load considered in the stabilizing moment are measured orthogonally to the above-mentioned axis passing by the hinge A and it is evaluated as follows:

$$d_j = \frac{\sqrt{2}}{2}(b_j-a_j)+\sqrt{2}s \tag{10}$$

being a_j and b_j the distances of the j-th vertical load point of application from the corner angle (see Fig. 3) measured in the horizontal and vertical direction, respectively.

2.3. Seismic assessment: capacity versus demand

To carry out the safety assessment on the local collapse mechanism it must be checked whether the acceleration capacity of the mechanism, hereinafter labeled as a_C is enough to stand the associated demand which depends on the site's expected acceleration. Specifically, the Italian Technical Code (Decreto 17 gennaio 2018, 2018) (in the sequel simply referred to as NTC, 2018) defines the acceleration capacity as follows:

$$a_C = \frac{\alpha_0 g}{e^* \text{CF}} \tag{11}$$

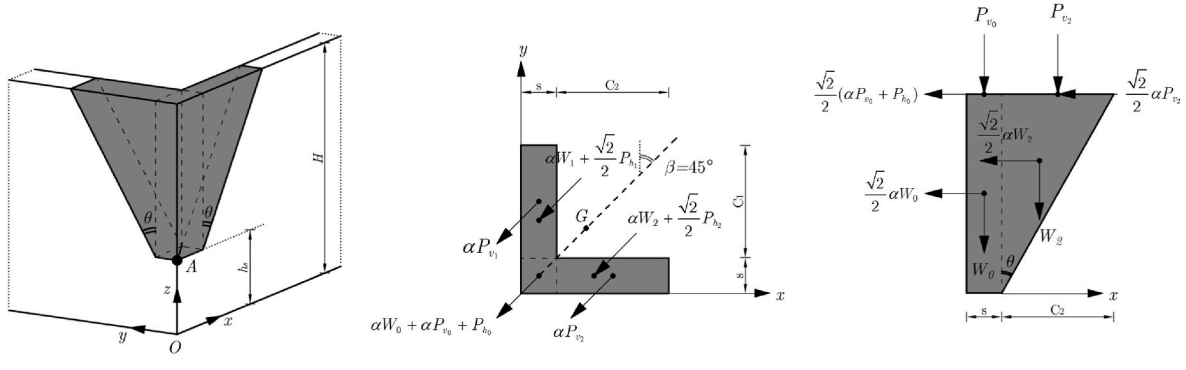

Fig. 2. Corner overturning mechanism: (a) 3D view, (b) plane view and (c) lateral view.

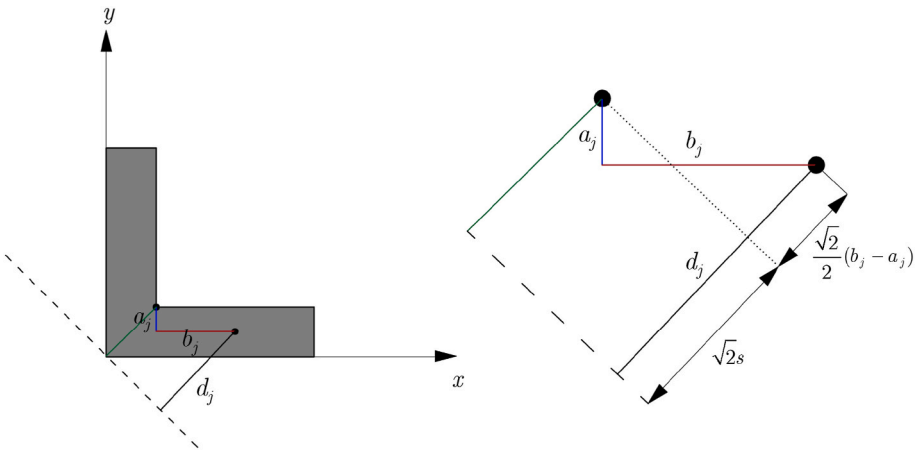

Fig. 3. Scheme for the evaluation of lever arms in the overturning mechanism.

where α_0 is the minimum load multiplier that triggers the mechanism activation, CF is a confidence factor that accounts for the available level of knowledge of the structure and e^* is the participating fraction mass expressed as the ratio between the modal mass and the total mass of the portion involved in the mechanism.

Even though the deterministic safety assessment is carried out, according to the NTC 2018, by considering in Eq. (11) the minimum load multiplier α_0, it is worth noting that in the present paper, to study the effect of the uncertainties on the acceleration capacity assessment, only the functional relation contained in Eq. (11) is adopted for its evaluation. Therefore, the independent variable α, representative of the load multiplier function obtained via PVW, is considered in the analysis in place of α_0. It follows that, for safety assessment purposes, the region of interest for the actual acceleration capacity associated with the specific local mechanism is found approaching its minimum value.

On the other hand, the acceleration demand is defined in terms of the significant vibrational modes of the structure. The acceleration contribution related to the k-th mode at the floor height z is defined as:

$$a_{zk}(z) = S_e(T_k, \xi_k)\gamma_k \psi_k(z)\sqrt{1 + 0.0004\xi_k^2} \tag{12}$$

where $S_e(T_k, \xi_k)$ is the k-th mode spectral acceleration (defined for the specific limit state analyzed) for the k-th natural period T_k and damping coefficient ξ_k (which is generally assumed equal to 5%), γ_k is the k-th mode's participation factor and $\psi_k(z)$ is the value assumed by the k-th modal vector at the height z. The acceleration demand is therefore evaluated as the sum of modal contributions:

$$a_D = \frac{\sqrt{\sum_k (a_{zk}(z))^2}}{q} \tag{13}$$

where q is the behavior factor which assumes the values of 1 for serviceability limits state (SLS) and 2 for ultimate limit states (ULS). The safety verification with respect to the local mechanism is attained if it is verified that $a_C > a_D$. It is worth noticing that, in most cases for masonry structures it is enough to consider only the first mode contribution, and the following expression is proposed by the technical code for the modal participation factor:

$$\gamma_1 = \frac{3n}{2n+1} \tag{14}$$

where n is the number of floors.

3. Uncertainties in the out-of-plane local failure mechanisms

Since the local mechanism activation could be significantly influenced by the effect of uncertainties, it is advisable to introduce uncertain parameters in the failure mechanism model. Specifically in the case of the vertical bending mechanism the main uncertainties which may affect the kinematic analysis are contained in the masonry specific weight γ as well as in the exact location μ where the cylindrical hinge is formed. Further, when the corner overturning mechanism is considered an additional uncertain parameter θ related to the inclination of crack lines with respect to the vertical direction must be considered. To this aim, the above-mentioned quantities are represented as uncertain parameters with a constant mean value and a dimensionless deviation according to the expressions:

$$\gamma = \gamma_m(1 + \chi) \tag{15a}$$

$$\mu = \mu_m(1 + \epsilon) \tag{15b}$$

$$\theta = \theta_m(1 + \delta) \tag{15c}$$

where γ_m, μ_m and θ_m represent the mean value of the specific weight, horizontal cylindrical hinge position and crack line inclination, respectively. Further, χ, ε and δ specify the corresponding symmetric dimensionless fluctuations.

Aiming to compare two different formulations to account for the uncertainties effect on the load multiplier α as well as on the corresponding uncertain acceleration capacity a_C, the basic notations for the two models considered in this study are introduced in the following. In the first approach, the uncertain parameters are represented as random variables with the assigned PDF. Specifically, by assuming the symmetric fluctuations χ, ε and δ as zero-mean stochastic variables, Eq. (3) can be rewritten in the form:

$$\widehat{\gamma} = \gamma_m(1 + \widehat{\chi}) \tag{16a}$$

$$\widehat{\mu} = \mu_m(1 + \widehat{\epsilon}) \tag{16b}$$

$$\widehat{\theta} = \theta_m(1 + \widehat{\delta}) \tag{16c}$$

with $\gamma_m = E\langle\widehat{\gamma}\rangle$, $\mu_m = E\langle\widehat{\mu}\rangle$ and $\theta_m = E\langle\widehat{\theta}\rangle$, the mean values of the masonry specific weight, hinge position and crack lines inclination, respectively. It is worth specifying that the symbol "$\widehat{\cdot}$" over a variable denotes a stochastic quantity, whereas $E\langle\cdot\rangle$ is the stochastic average operator. In order to guarantee positive values of $\widehat{\gamma}$, $\widehat{\mu}$ and $\widehat{\theta}$, the random variables $\widehat{\chi}$, $\widehat{\epsilon}$ and $\widehat{\delta}$ must satisfy the restriction $|\widehat{\chi}| < 1$, $|\widehat{\epsilon}| < 1$ and $|\widehat{\delta}| < 1$, with $|\cdot|$ denoting the absolute value.

On the other hand, in the second proposed model, the uncertainties are described by interval or uncertain-but-bounded variables. Following the interval analysis formalism, the generic k-th interval variable may be interpreted as a bounded real number x_k such that $x_k^I \triangleq [\underline{x}_k, \overline{x}_k] \in \mathbb{R}$ where

the superscript I refers to the interval variable whereas $\underline{x}_k$ and $\overline{x}_k$ represent its lower bound (LB) and upper bound (UB), respectively. Specifically, under the assumption of symmetrical intervals, the interval variable may be expressed in terms of its central value $x_{m,k}$ and its deviation Δx_k:

$$x_k^I = \left[x_{m,k} - \Delta x_k, x_{m,k} + \Delta x_k\right] = x_{m,k} + \Delta x_k e_{x,k}^I \tag{17}$$

with

$$x_{m,k} = \frac{\underline{x}_k + \overline{x}_k}{2}; \quad \Delta x_k = \frac{\overline{x}_k - \underline{x}_k}{2}; \quad e_{x,k}^I \triangleq [-1, 1] \tag{18}$$

It follows that the uncertain variable x_k^I can be rewritten as

$$x_k^I = x_{m,k}\left(1 + \xi_k^I\right) \tag{19}$$

where $\xi_k^I = \Delta\xi_k e_{\xi,k}^I$, defined in terms of $\Delta\xi_k = \Delta x_k / x_{m,k}$ and $e_{\xi,k}^I \triangleq [-1,1]$, is the normalized fluctuation around $x_{m,k}$. Following the aforementioned notation, the uncertain-but-bounded parameters considered in this study are written as follows:

$$\gamma^I = \gamma_m(1 + \chi^I) = \gamma_m(1 + \Delta\chi e_\chi^I) \tag{20a}$$

$$\mu^I = \mu_m(1 + \epsilon^I) = \mu_m(1 + \Delta\epsilon e_\epsilon^I) \tag{20b}$$

$$\theta^I = \theta_m(1 + \delta^I) = \theta_m(1 + \Delta\delta e_\delta^I) \tag{20c}$$

In Eq. (3), the γ_m, μ_m and θ_m represent the central values of the uncertain variables in input matching with the deterministic nominal values for the specific weight, the position of the horizontal cylindrical hinge and the crack inclination mean values, respectively; $\Delta\chi = \Delta\gamma/\gamma_m$, $\Delta\varepsilon = \Delta\mu/\mu_m$ and $\Delta\delta = \Delta\theta/\theta_m$ denote the fluctuations of the uncertain parameters around their nominal values. The unitary intervals e_χ^I, e_ϵ^I and e_δ^I allow treating variables with multiple occurrences of the same type as dependent ones (Muscolino and Sofi, 2012).

The two aforementioned modeling approaches to study the effect of uncertainties have been recently compared in (Laudani and Santoro, 2022). Specifically, an extensive comparative analysis linked, for the first time, the response PDF with the response interval bounds. The authors found out that the response interval, defined through the upper and the lower bounds response values ($\underline{x}$ and $\overline{x}$, respectively), satisfies the following property:

$$\int_{\underline{x}}^{\overline{x}} p_x(x)dx = Pr[\underline{x} < x < \overline{x}] \approx 1 \tag{21}$$

The above equation guarantees that the PDF $p_x(x)$ is defined in the interval $[\underline{x}, \overline{x}]$ and outside this range it assumes negligible values (see Fig. 4). That result gave a new perspective on the comparison between estimates derived by probabilistic and interval analyses for which, in different existing literature studies, divergent results have been presented. In addition, the authors prove that the above property does not depend on the kind of assumption of the joint PDF of the random parameters involved (Muscolino et al., 2013; Sofi, 2015; Santoro and Muscolino, 2019).

3.1. PDF of the seismic response for the out-of-plane mechanism

Adopting a stochastic approach, the PDF of the response function (alternatively the load multiplier α or the acceleration capacity a_C) can be determined by adopting the Probability Transformation Method (PTM) (Laudani and Falsone, 2021; Falsone and Laudani, 2020). It stems from the concept of random variable space transformation and the probability conservation principle (Li and Chen, 2009). Specifically, let $\mathbf{x}$ be a n-dimensional vector with known joint probability density function $p_{\mathbf{X}}(\mathbf{x})$ and $\mathbf{h}$ an invertible n-dimensional functional relation whose inverse is $\mathbf{h}^{-1}(\cdot) = \mathbf{g}(\cdot)$. In this specific case, the load multiplier α and the acceleration capacity a_C form the output vector and their functional relations with the input uncertain parameters have been presented in Section 2 and 3. Assuming $\mathbf{w} = \mathbf{h}(\mathbf{x})$ as the random vector of the output it is possible to evaluate its joint probability density function as follows:

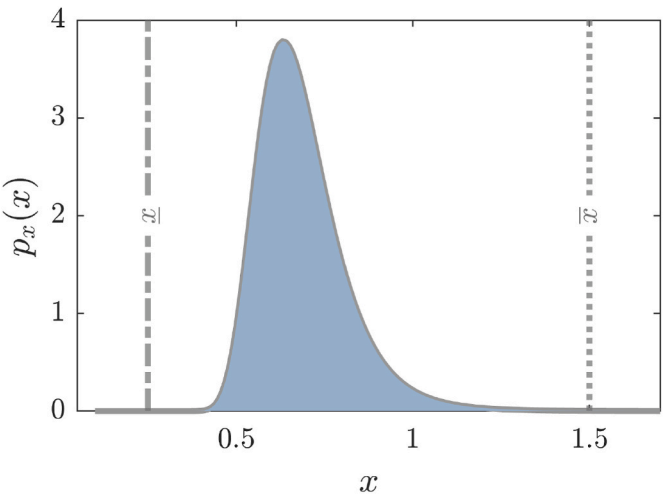

Fig. 4. Explanatory figure of the results provided by the comparative analysis: lower bound $\underline{x}$ and upper bound $\overline{x}$ of the generic response function x evaluated via interval procedures represent the extremes for which the PDF response function $p_x(x)$ has numerical significance.

$$p_{\mathbf{W}}(\mathbf{w}) = \frac{1}{|\det[\mathbf{J}_{\mathbf{h}}(\mathbf{g}(\mathbf{w}))]|} p_{\mathbf{X}}(\mathbf{g}(\mathbf{w})) = \left|\det\left[\mathbf{J}_{\mathbf{g}}(\mathbf{w})\right]\right| p_{\mathbf{X}}(\mathbf{g}(\mathbf{w})) \tag{22}$$

where $\mathbf{J}_{\mathbf{h}}(\cdot)$ and $\mathbf{J}_{\mathbf{g}}(\cdot)$ represent the Jacobian matrices associated with the direct relation $\mathbf{w} = \mathbf{h}(\mathbf{x})$ and the inverse one $\mathbf{x} = \mathbf{g}(\mathbf{w})$.

From a probabilistic point of view, the considered uncertain parameters are statistically uncorrelated: therefore, to properly carry out a suitable comparison between the two approaches, it is reasonable to assume that the input vector $\mathbf{x} = [\widehat{\gamma} \quad \widehat{\mu} \quad \widehat{\theta}]$ is made up of independently distributed variables.

3.2. Bounds of the seismic response for the out-of-plane mechanism

Under the assumption of uncertain parameters described as interval variables, it follows that also the response variables associated with the local mechanism, namely the load multiplier α and the acceleration capacity a_C, become in turn interval variables functions:

$$\begin{aligned} \alpha^I &= \alpha(\gamma^I, \mu^I, \theta^I) \\ a_C^I &= a_C(\gamma^I, \mu^I, \theta^I) \end{aligned} \tag{23}$$

The closed analytical forms of the response functions (see e.g. Eqs.(3) and (5)–(6)) with their explicit dependence on the uncertain-but-bounded parameters allow evaluating the range of the local mechanism responses variability by simply adopting the global optimization (GO) procedure. Specifically, upper and lower bounds of the response functions may be attained through the solution of the following constrained problems:

$$\begin{cases} \underline{\alpha} = \text{minimize}\left[\alpha(\gamma^I, \mu^I, \theta^I)\right] \\ \text{subjected to} \\ \gamma \in \left[\underline{\gamma}, \overline{\gamma}\right], \mu \in \left[\underline{\mu}, \overline{\mu}\right], \theta \in [\underline{\theta}, \overline{\theta}] \end{cases} \tag{24}$$

$$\begin{cases} \overline{\alpha} = \text{maximize}\left[\alpha(\gamma^I, \mu^I, \theta^I)\right] \\ \text{subjected to} \\ \gamma \in \left[\underline{\gamma}, \overline{\gamma}\right], \mu \in \left[\underline{\mu}, \overline{\mu}\right], \theta \in [\underline{\theta}, \overline{\theta}] \end{cases} \tag{25}$$

where the uncertain parameters represent the design variables and the

intervals in which they are contained define the constraints for the variables. Similarly, the upper and lower bound for the acceleration capacity function a_C may be obtained properly by modifying Eq. (24)–(25) by substituting α with the other objective function a_C.

4. Numerical applications

In this section, the seismic analysis of the masonry local failure mechanisms in presence of uncertainties is presented. Following both probabilistic and non-probabilistic approaches, the seismic response in terms of load multiplier α and acceleration capacity a_C is provided analyzing both the behavior of the vertical bending mechanism as well as the corner overturning mechanism. In particular, the stochastic analysis is carried out considering two alternative PDF distributions for the involved random parameters, namely the uniform distribution and the truncated normal distribution, hereinafter labeled as UD and TND respectively. Further, the results obtained taking into account the effect of the uncertainties on the acceleration capacity, are critically compared with normative code provisions which account for the model uncertainty in a simplified way through the confidence factor CF related to the level of knowledge about the structure. Specifically, three different CFs are considered, ranging from 1 to 1.35; the higher the level of knowledge available for the structure, the lower the CF factor will be. The safety assessment at the life-safety limit state (ULS) is also carried out by comparing the acceleration demand and the corresponding capacity (the latter is calculated with the above-mentioned procedures). To this aim, the acceleration demand is defined, according to the NTC 2018, once the seismic hazard parameters for the considered structure location are defined. Specifically in this study, it is assumed that the investigated local mechanisms are related to a masonry structure located in Messina (Italy) and the corresponding parameters necessary for the acceleration demand estimation, i.e. the maximum horizontal ground acceleration a_g, the maximum value of the amplification factor of the spectrum in horizontal acceleration F_0 and upper limit of the period at spectrum's constant speed in horizontal acceleration T_C^*, are summarized in Table 2.

4.1. Vertical bending mechanism in presence of uncertain parameters

In this subsection, the vertical bending mechanism is first investigated considering the uncertain positions of the horizontal cylindrical hinge as well as the uncertain specific weight. Specifically, the mechanical and geometrical characteristics assumed for the two blocks represented in Fig. 1 are summarized in Table 3. For the investigated mechanism, following the NTC2018 and assuming a B-type soil, the acceleration demand is assumed equal to 0.145 g. The analysis is addressed by assuming two different nominal positions of the horizontal cylindrical hinge.

In the first case herein considered, it is hypothesized that the horizontal cylindrical hinge could be formed at 0.5 h, thus the nominal value of the uncertain parameter μ_0 (see Eqs. 16b and 20b) is assumed equal to 2. Further, for the specific weight of the masonry γ, the nominal value γ_0 (see Eqs. 16a and 20a) is assumed equal to 1500 kg/m^3. In the framework of the stochastic model, the zero mean random fluctuations, $\widehat{\epsilon}$ and $\widehat{\chi}$, are assumed to possess alternatively UD and TND distribution on the intervals $[-0.2, 0.2]$ and $[-0.1, 0.1]$, respectively. While, by considering the interval model for the uncertainties, it is assumed a variation from the nominal hinge position $\Delta\varepsilon$ equal to 0.2 and a variation from the nominal specific weight $\Delta\chi$ equal to 0.1. In this damage configuration, the considered failure mechanism is represented in Fig. 1

Table 2
Reference values for seismic hazard parameters in Messina at the life-safety limit state (ULS).

	T_R	a_g	F_0	T_C^*
ULS	475	0.249 g	2.410	0.360

Table 3
Geometry and load parameters assumed in the numerical analysis of the vertical bending failure mechanism.

Geometry	
h	3.2 m
t	0.5 m
L	1.1 m
e	0 m
h_s	2.2 m
Loads	
N	3145 kg
P	1845 kg
S	1060 kg

(a) and Eq. (3) holds. The two applied procedures, i.e. the probabilistic approach (through the PTM) and the interval one (through the GO technique), allow to estimate the PDF and the bounds, respectively, of the uncertain activation multiplier α as well as of the uncertain acceleration capacity a_C. Once LB and UB of the load multiplier α and the acceleration capacity a_C are evaluated, their central values are calculated as

$$\alpha_m = \frac{\underline{\alpha} + \overline{\alpha}}{2}; \quad a_{Cm} = \frac{\underline{a}_{Cm} + \overline{a}_{Cm}}{2} \tag{26}$$

Figs. 5 and 6 show the PDF of the activation multiplier, $p_\alpha(\alpha)$, and of the acceleration $p_{a_C}(a_C)$ through the PTM application compared with the corresponding LB and UB provided by the interval analysis. In both cases, the close link between the two investigated approaches to treat the uncertainties in the model is evident in the graphics.

Further, Fig. 6 shows that regardless of the selected approach, the safety assessment is by far satisfied. Notably, a good agreement is observed between the NTC 2018 and the proposed approaches since the estimates calculated with the technical code fall in the domain spanned by the evaluated PDFs.

From the observation of Figs. 5 and 6, it is noted that the obtained PDFs are significantly asymmetrical regardless of the adopted distribution. It follows that the central values of the load multiplier as well as the capacity acceleration differ significantly from their mean values for both "UD" and "TND". This behavior is due to the nonlinear relationship between input and output variables. Furthermore, the central values considered in these figures are obtained as the average of the UB and LB of each response function (see Eq. (18)) as previously highlighted. It is remarked that, in general, the output interval of the response function could be not symmetric.

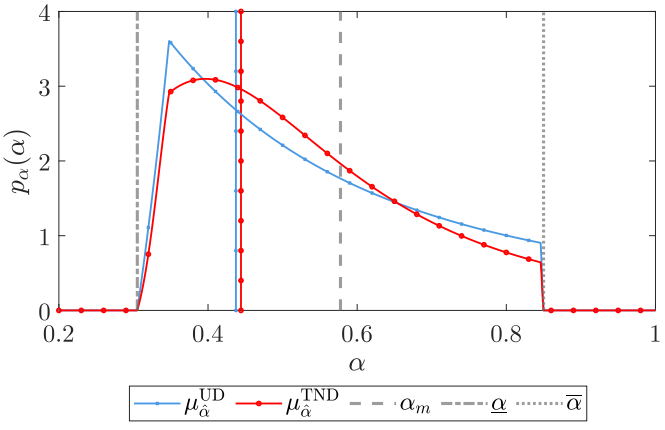

Fig. 5. Vertical bending failure mechanism assuming the horizontal cylindrical hinge at $h_1 = 0.5h$: LB, UB and PDFs of the load multiplier α. The additional vertical lines represent the central value of the load multiplier α_m (dashed line) and the mean values μ_α of the two PDFs (lines with markers).

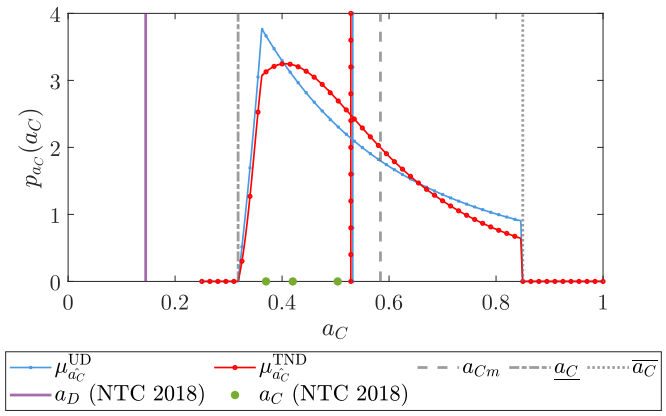

Fig. 6. Vertical bending failure mechanism assuming the horizontal cylindrical hinge at $h_1 = 0.5h$: LB, UB and PDFs of the acceleration capacity a_C. The additional vertical lines represent the central value of the acceleration capacity a_{Cm} (dashed line) and the mean values μ_{a_C} of the two PDFs (lines with markers). NTC 2018 provisions are represented in terms of acceleration capacity (green dots) and demand (purple line). (For interpretation of the references to colour in this figure legend, the reader is referred to the Web version of this article.)

Taking full advantage of the results of the stochastic analysis a further investigation is conducted to better understand the role of the uncertainties in the kinematic model considering both the separate and combined influence of each uncertain parameter. To this end, for different values of the standard deviation of the uncertain input parameters (σ_μ and σ_γ), alternatively assuming that they are uniformly distributed (UD) or a truncated normally distributed (TND), the coefficients of variation associated with the load multiplier α and acceleration capacity a_C, namely $\mathrm{COV}_i = \sigma_i/\mu_i$ (with $i = \alpha, a_C$), have been evaluated. From the results reported in Table 4 it is noted how the uncertainty on the position of the horizontal cylindrical hinge μ has a non-negligible influence on the response functions in comparison with the effect of uncertainty on specific weight γ. It may be also noted how, accounting for the combined effect of the uncertainties on the hinge position μ and the specific weight γ, the degree of uncertainties produced on the response is amplified with COVs up to 62.17% for the load multiplier and 26.3% for the acceleration capacity, respectively.

Moreover, in Table 4 the percentage difference between mean and central values of the acceleration capacity (i.e. $\Delta_{|a_{Cm}-\mu_{a_C}|} = (|a_{Cm} - \mu_{a_C}|/a_{Cm}) * 100$) is reported considering both the combined and separate effect of different levels of uncertain parameters. Specifically, in the case when the uncertainty is on the position of the hinge μ as well as in the case when both hinge position μ and the specific weight γ are uncertain, it is possible to note a percentage difference up to around 10% between mean and center values of the acceleration capacity. The high values of the percentage difference demonstrate the significant nonlinear relationship between input uncertain parameters and acceleration capacity. Therefore, even if these comparative analyses confirm that the interval defined by lower and upper bounds represents the entire significant space of the probability density function, the probabilistic method is highly recommended for an exhaustive stochastic analysis.

In the following, the second kinematic chain configuration (see Fig. 1 (b)) is analyzed with the only modification on the nominal position of the horizontal cylindrical hinge and leaving unaltered all the other data. Specifically, it is hypothesized that the horizontal cylindrical hinge could be activated at $h_1 = 0.75\,h$, thus the nominal value of the uncertain parameter is $\mu_0 = 4$. The same assumptions to describe the uncertain parameters have been confirmed in this second case study; namely UD and TND distributions in the intervals $[-0.2, 0.2]$ and $[-0.1, 0.1]$ for the random variables $\widehat{\varepsilon}$ and $\widehat{\chi}$, respectively, and $\Delta\varepsilon = 0.2$ and $\Delta\chi = 0.1$ for the interval variables ε^I and χ^I.

In this second scenario, the expressions for the PWV as well for the load multiplier α are referred to the Case 2. Therefore, in Fig. 7 the LB, UB and PDFs of the activation multiplier α are reported. The outputs of the two methods related to the acceleration a_C are shown in Fig. 8. In this case, it's worth noting that the estimated PDFs for both the load multiplier α and the acceleration capacity a_C contrary to the previous case present a symmetry leading to mean values closer to the center value. This result is related to the different expression provided for the PVW due to the new position of the cylindrical hinge with respect to the application point of the horizontal loads assumed in the kinematic model (see Fig. 1(b) and Eq. (5)) where the nonlinearity aspect is less evident. Once again in both cases, the two investigated methodologies confirmed the expected results (see Eq. (21)).

However, contrary to the previous case, Fig. 8 shows that even though the safety assessment is satisfied according to the normative provisions regardless of the specific value of CF, the same does not happen if the proposed approach is instead adopted since both the lower bound and part of the PDF functions of the acceleration capacity provides values lower than the corresponding acceleration demand. This is specifically significant since the acceleration capacity range for which the safety assessment is not satisfied corresponds to the range of the

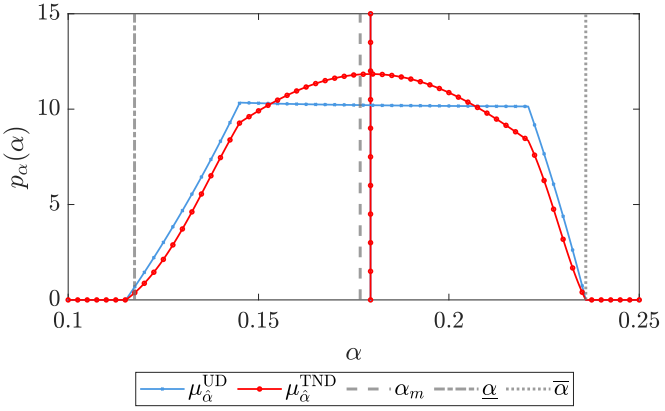

Fig. 7. Vertical bending mechanism analysis assuming the hinge at $h_1 = 0.75h$: LB, UB and PDFs of the load multiplier α. The additional vertical lines represent the central value of the load multiplier α_m (dashed line) and the mean values μ_α of the two PDFs (lines with markers).

Table 4
Vertical bending failure mechanism assuming the horizontal cylindrical hinge at $h_1 = 0.5h$: statistical characterization of the kinematic model considering both the separate and combined effect of the uncertain parameters μ and γ on the response functions α and a_C in terms of COV percentage and difference between mean and central acceleration capacity values.

	Uncertainty on μ				Uncertainty on γ				Combined uncertainties			
	UD ($\sigma_\mu = 0.1$)	TND ($\sigma_\mu = 0.1$)	UD ($\sigma_\mu = 0.2$)	TND ($\sigma_\mu = 0.2$)	UD ($\sigma_\gamma = 0.1$)	TND ($\sigma_\gamma = 0.1$)	UD ($\sigma_\gamma = 0.2$)	TND ($\sigma_\gamma = 0.2$)	UD ($\sigma_{\mu,\gamma} = 0.1$)	TND ($\sigma_{\mu,\gamma} = 0.1$)	UD ($\sigma_{\mu,\gamma} = 0.2$)	TND ($\sigma_{\mu,\gamma} = 0.2$)
COV_α [%]	13.17	12.32	27.31	25.58	0.81	0.76	1.64	1.53	16.15	14.41	62.17	57.37
COV_{a_C} [%]	14.65	13.40	27.20	25.25	5.31	4.30	7.70	6.63	12.64	11.79	26.31	24.63
$\Delta_{\lvert a_{Cm}-\mu_{a_C}\rvert}$ [%]	3.21	3.24	11.35	11.82	0.23	0.13	0.37	0.20	2.02	2.16	8.85	9.48

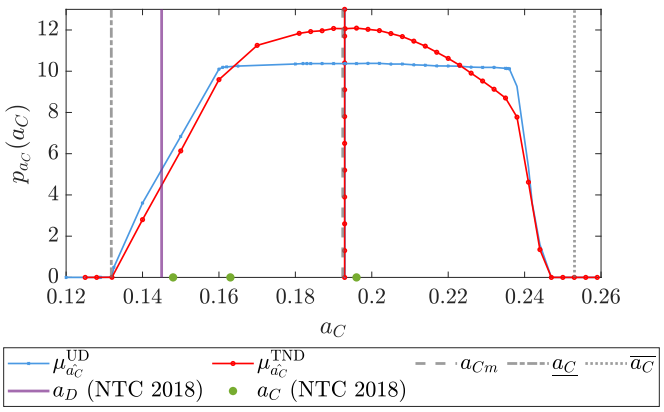

Fig. 8. Vertical bending mechanism analysis assuming the hinge at $h_1 = 0.75h$: LB, UB and PDFs of the acceleration capacity a_C. The additional vertical lines represent the central value of the acceleration capacity a_{Cm} (dashed line) and the mean values μ_{a_C} of the two PDFs (lines with markers). NTC 2018 provisions are represented in terms of acceleration capacity (green dots) and demand (purple line). (For interpretation of the references to colour in this figure legend, the reader is referred to the Web version of this article.)

smallest load multipliers which, hence, have the highest probability of being triggered due to a seismic event. This, in turn, depends on the choice to exploit the NTC 2018 functional relation for the acceleration capacity, adopting as α the expression obtained using the kinematic analysis, as mentioned in Section 3. Similarly to the previous case, a statistical study on the effect of uncertainties has been carried out and results are reported in Table 5. Specifically, it is observed that in this case the uncertain parameters have a comparable influence on the response functions with COVs up to 10.1% and 12.7% for the separate effect of the hinge position and the specific weight, respectively. Once again it is noted that, considering both uncertain parameters, COVs significantly increase up to 51.3% and 14.9% for the load multiplier and the acceleration capacity, respectively. It is also worth noting that the highest observed percentage difference between the mean and central values for the acceleration capacity is 2.59% considering the combined effect of the uncertainties on μ and γ in the uniform distribution; on the other hand, in the previous investigated case, the highest percentage difference (11.82%) was attained considering only the effect of the uncertainties on μ. Contrary to the previous case, the low values of the percentage difference allow us to draw that a non-probabilistic analysis, in terms of interval bounds of the acceleration capacity, could be comprehensive for the investigated problem.

4.2. Corner overturning mechanism in presence of uncertain parameters

This subsection aims to study the effect of the uncertainties on the corner overturning mechanism. The proposed case study deals with a masonry structure covered by a hipped roof. Specifically, the latter is characterized by hip rafters leaning on the corners of the building and rising to the central ridge; this solution does not produce horizontal forces on the converging walls focusing the thrust effect only at the corner via the hipped rafters. In the considered case study no openings are present near the corner and the involved walls have the same masonry material and thickness, thus the crack line inclination is symmetric in both walls (see Fig. 2). The loads considered in the kinematic models include the weight of the masonry blocks, the distributed load q that takes into account the gravity loads of the roof, the point load exerted by the hip rafter at the intersection of the walls P_v and the corresponding horizontal thrust P_h. The geometric properties and loads for the investigated local mechanism are summarized in Table 6. In this application, the effect of the uncertainties is considered on the crack lines inclination θ whose nominal value θ_0 is assumed $\pi/6$ with respect to the vertical direction, the specific weight of masonry γ, whose nominal value γ_0 is assumed 1500 kg/m^3 and the position at which the hinge is formed μ for which the corresponding nominal value μ_0 is determined assuming a nominal height value of $h_{s_0} = 2.15$ m. Assuming once again that the structure is located in Messina with the same type of soil considered in the previous case, the acceleration demand associated with the local mechanism for the life-safety state limit is equal to 0.183 g.

Table 6
Geometry and load parameters assumed in the numerical analysis of the corner overturning failure mechanism.

Geometry	
h	4.3 m
t	0.3 m
h_s	2.15 m
Loads	
P_v	2478 kg
P_h	190.6 kg
q	1835 kg/m

Regarding the description of the uncertain parameters, in the stochastic model the zero mean random fluctuation $\widehat{\epsilon}$ is assumed to possess alternatively UD and TND distribution on the interval $[-0.2, 0.2]$, similar considerations hold for both $\widehat{\delta}$ and $\widehat{\chi}$ in the interval $[-0.1, 0.1]$; in the interval model for the uncertainties it is assumed $\Delta\epsilon = 0.2$ for the hinge position and $\Delta\delta = \Delta\chi = 0.1$ for both the crack line inclination and the specific weight.

The results of the two investigated approaches are reported in Figs. 9 and 10 confirming again a good agreement between the probabilistic and non-probabilistic approaches for the effect of uncertainties on the corner overturning kinematic model. However, it is noted in Fig. 10 that, when adopting the stochastic approach, the safety assessment is not always satisfied, especially in the case of acceleration capacities corresponding to lower values of load multiplier; it is also highlighted how the simplified normative approach reaches similar results only if a poor degree of knowledge is assumed for the structure and, thus, a high CF value is chosen.

The results of the statistical analysis, carried out considering both the separate and combined effects of the three investigated uncertainties μ, γ and θ, are summarized in Tables 7 and 8, respectively. It is noted how the effect of uncertainty on the crack line inclination θ is more significant (highest COV of 12.81%) for this mechanism in comparison with the

Table 5
Vertical bending failure mechanism assuming the horizontal cylindrical hinge at $h_1 = 0.75h$: statistical characterization of the kinematic model considering both the separate and combined effect of the uncertain parameters μ and γ on the response functions α and a_C in terms of COV percentage and difference between mean and central acceleration capacity values.

	Uncertainty on μ				Uncertainty on γ				Combined uncertainties			
	UD ($\sigma_\mu = 0.1$)	TND ($\sigma_\mu = 0.1$)	UD ($\sigma_\mu = 0.2$)	TND ($\sigma_\mu = 0.2$)	UD ($\sigma_\gamma = 0.1$)	TND ($\sigma_\gamma = 0.1$)	UD ($\sigma_\gamma = 0.2$)	TND ($\sigma_\gamma = 0.2$)	UD ($\sigma_{\mu,\gamma} = 0.1$)	TND ($\sigma_{\mu,\gamma} = 0.1$)	UD ($\sigma_{\mu,\gamma} = 0.2$)	TND ($\sigma_{\mu,\gamma} = 0.2$)
COV_α [%]	5.26	4.91	9.98	9.43	3.61	6.13	7.08	12.69	6.33	5.92	51.30	47.92
COV_{a_C} [%]	6.99	6.38	10.08	9.39	4.61	3.83	9.88	8.79	5.90	5.49	14.85	12.28
$\Delta_{\lvert a_{Cm} - \mu_{a_C} \rvert}$ [%]	0.36	0.30	0.47	0.49	0.07	0.11	0.19	0.38	0.77	0.78	2.59	1.00

Table 7
Corner overturning failure mechanism: statistical characterization of the kinematic model considering the separate effect of the uncertain parameters μ, γ and θ on the response functions α and a_C in terms of COV percentage and difference between mean and central acceleration capacity values.

	Uncertainty on μ				Uncertainty on γ				Uncertainty on θ			
	UD	TND	UD	TND	UD	TND	UD	TND	UD	TND	UD	TND
	($\sigma_\mu = 0.1$)		($\sigma_\mu = 0.2$)		($\sigma_\gamma = 0.1$)		($\sigma_\gamma = 0.2$)		($\sigma_\theta = 0.1$)		($\sigma_\theta = 0.2$)	
COV_α [%]	4.71	3.96	3.80	3.69	2.18	2.05	3.83	3.35	7.98	6.98	14.11	12.81
COV_{a_C} [%]	3.35	3.11	9.26	7.92	8.81	7.63	1.30	1.72	9.00	7.66	11.86	11.13
$\Delta_{\lvert a_{Cm} - \mu_{a_C} \rvert}$ [%]	0.29	0.28	1.53	1.35	0.33	0.30	0.81	0.58	0.73	0.56	1.08	1.09

Table 8
Corner overturning failure mechanism: statistical characterization of the kinematic model considering the combined effect of the uncertain parameters μ, γ and θ on the response functions α and a_C in terms of COV percentage and difference between mean and central acceleration capacity values.

	Combined uncertainties			
	UD	TND	UD	TND
	($\sigma_{\mu,\gamma,\theta} = 0.1$)		($\sigma_{\mu,\gamma,\theta} = 0.2$)	
COV_α [%]	5.93	5.55	11.79	12.93
COV_{a_C} [%]	5.51	5.69	9.19	7.58
$\Delta_{\lvert a_{Cm} - \mu_{a_C} \rvert}$ [%]	1.85	1.91	3.07	3.77

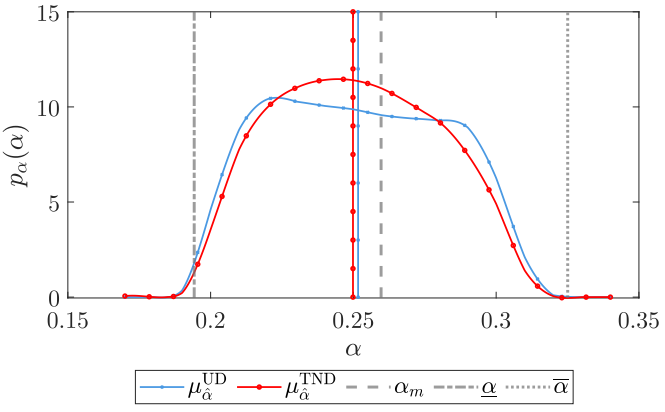

Fig. 9. Corner overturning failure mechanism: LB, UB and PDFs of the load multiplier α. The additional vertical lines represent the central value of the load multiplier α_m (dashed line) and the mean values μ_α of the two PDFs (lines with markers).

other two remaining parameters, namely μ and γ. It is also worth noticing that, in this specific case, the combined effect of the uncertainties on the above-mentioned parameters does not produce a relevant amplification of the COV whose maximum value is 12.93% for the investigated type of probability distribution (TND) and standard deviation input uncertain parameters. Finally, regarding the results of the percentage difference between the mean and central values of the acceleration capacity, it is possible to appreciate that in the analyses for which only one uncertain parameter is involved the percentage difference is almost lower than 1%. Therefore, the expeditious interval analysis could be sufficient. However, if the combined effect of the uncertain parameters μ, γ and θ on the response function a_C is considered, percentage differences up to around 3% can be found, then the application of the probability method is recommended for a fully stochastic analysis.

5. A real case-study for a corner overturning failure mechanism

This section deals with the local collapse analysis of a real masonry building addressing the effects of uncertainties in the seismic safety assessment. The studied two-story structure is a primary school located

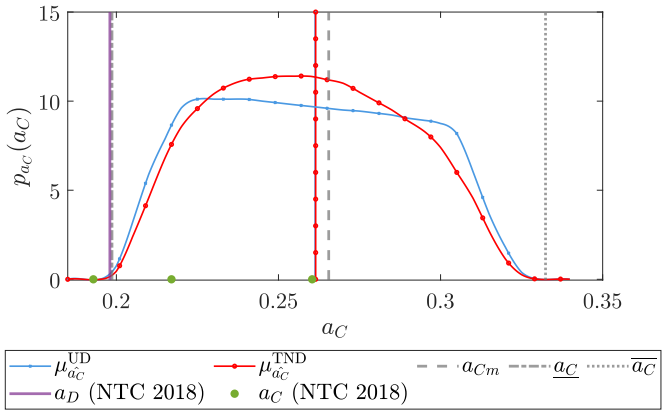

Fig. 10. Corner overturning failure mechanism: LB, UB and PDFs of the acceleration capacity a_C. The additional vertical lines represent the central value of the acceleration capacity a_{Cm} (dashed line) and the mean values μ_{a_C} of the two PDFs (lines with markers). NTC 2018 provisions are represented in terms of acceleration capacity (green dots) and demand (purple line). (For interpretation of the references to colour in this figure legend, the reader is referred to the Web version of this article.)

in Visso (Macerata province, Italy) affected by the 2016–2017 Central Italy earthquake sequence. Among the damages that occurred in the building, the attention is focused on the local overturning of the north corner (see Fig. 11) due to the lack of rigid connection with the timber roof. Besides, it is pointed out that the same structure has already been investigated in previous studies. Specifically, the same failure mechanism has already been discussed in the deterministic framework considering the traditional linear kinematic analysis in (Argiento et al.,

Fig. 11. Out-of-plane failure mechanism of the north corner of the primary school in Visso (Macerata, Italy).

2019), also including the effect of frictional forces, and via the non-linear dynamic approach, which accounts for the one-sided motion of the macro-block over time, in (Casapulla et al., 2019).

As it is shown in Fig. 11, the actual out-of-plane mechanism involved the formation of a single crack on one wall and, due to the presence of a window close to the corner, two main cracks on the remaining one, whose inclinations are labeled θ_1, θ_2 and θ_3, respectively (see Fig. 12(a)). Further, due to the timber roof conformation, i.e. ensemble of rafter and purlins supported by a system of beams, the walls of the structure were loaded by uniformly distributed loads, i.e. q_1 and q_2, whereas the hip rafter directly affected the corner with a concentrated inclined load whose components in the vertical and horizontal directions are T_{s0} and W_{s0}, respectively.

The loads considered in the macro-block analysis, shown in Fig. 12 (b), are the self-weights of the masonry walls, i.e. W_0, W_1 and W_2, the resultants of the distributed loads due to the roof, i.e. $W_{s1} = q_1 C_1$ and $W_{s2} = q_2(C_p + C_t)$, the components of the hip rafter weight, T_{s0} and W_{s0}, and the horizontal forces obtained by amplifying all the previously mentioned weights by the load multiplier α. Table 9 summarizes the deterministic parameters assumed for the analysis in terms of the geometry of the mechanism, masonry properties and loads. More detailed information on these parameters as well as the application of the PVW for this specific case may be found in (Argiento et al., 2019; Casapulla et al., 2019). In this case study, once again the effect of uncertainties is introduced on the masonry specific weight γ, the position of the hinge $\mu = H$ and the inclination of the crack lines θ. In this regard, it is noted that, for the macro-block formation, the presence of a window close to the corner in one of the walls forces the crack inclination θ_2 in the lower spandrel on the direction that connects the hinge and the lower corner of the opening (see Fig. 12(a)). However, it is also pointed out that the introduction of the uncertainty on the hinge position indirectly affects θ_2 making it also an uncertain parameter. On the other hand, the formation of the cracks in the upper spandrel and the other wall is not influenced by the openings and the uncertainty in their inclinations is taken into account assuming θ_3 and θ_1 as uncertain parameters, respectively. The uncertainties on both the hinge position and the crack line inclinations, together with the uncertainty on the material, directly affect the geometry of the macroblock thus making the weight contributions W_i ($i = 0, 1, 2$) uncertain quantities. Further, to conduct the analysis, it is assumed that, in the stochastic approach, zero mean random fluctuations for all the uncertain parameters possess UD or TND distribution on the interval [-0.1, 0.1], alternatively. Similarly, adopting the interval model, a fluctuation of 10% with respect to the nominal value is adopted for every uncertain-but-bounded variable. Figs. 13 and 14 show the results between the compared approaches in terms of load multiplier α and acceleration capacity a_C. Once again, a good agreement is reached between the two methodologies, i.e. the PDFs are perfectly confined by the upper and the lower bound values.

Table 9
Deterministic values of the geometry, material properties and loads for the corner failure mechanism of the investigated structure.

Geometry and material properties							
H	4.35 m	h_t	1.35 m	h_m	1.95 m	C_p	0.9 m
t	0.65 m	$\theta_1 = \theta_3$	45°	θ_2	40.60°	γ	21 kN/m^3
Loads							
q_1	16.16 kN/m	q_2	19.62 kN/m	W_{s0}	24.27 kN	T_{s0}	1.87 kN

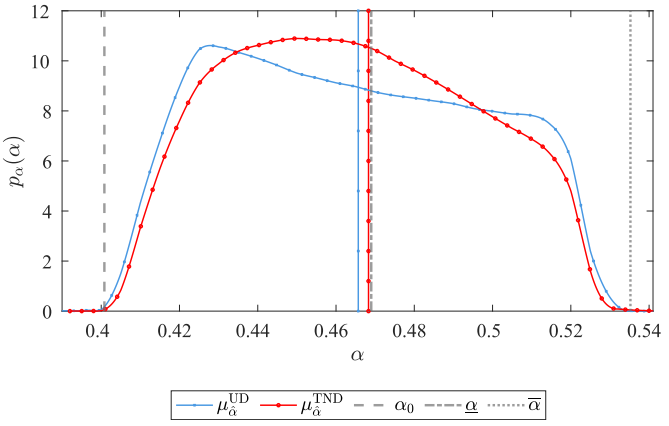

Fig. 13. Corner overturning failure mechanism in the primary school in Visso: LB, UB and PDFs of the load multiplier α. The additional vertical lines represent the central value of the load multiplier α_m (dashed line) and the mean values μ_α of the two PDFs (lines with markers).

While it is evident from Fig. 14 that the acceleration capacity's lower bound and a significant portion of its PDF functions yield values that are less than the corresponding acceleration demand. Furthermore, the safety assessment is not always achieved, particularly when the acceleration capacities correspond to lower load multiplier values. The authors specifically emphasize that it is straightforward to derive the explicit dependence on uncertain parameters of the seismic response in terms of load multiplier α and acceleration capacity a_C, as well as the application of the proposed procedures, even when the proposed

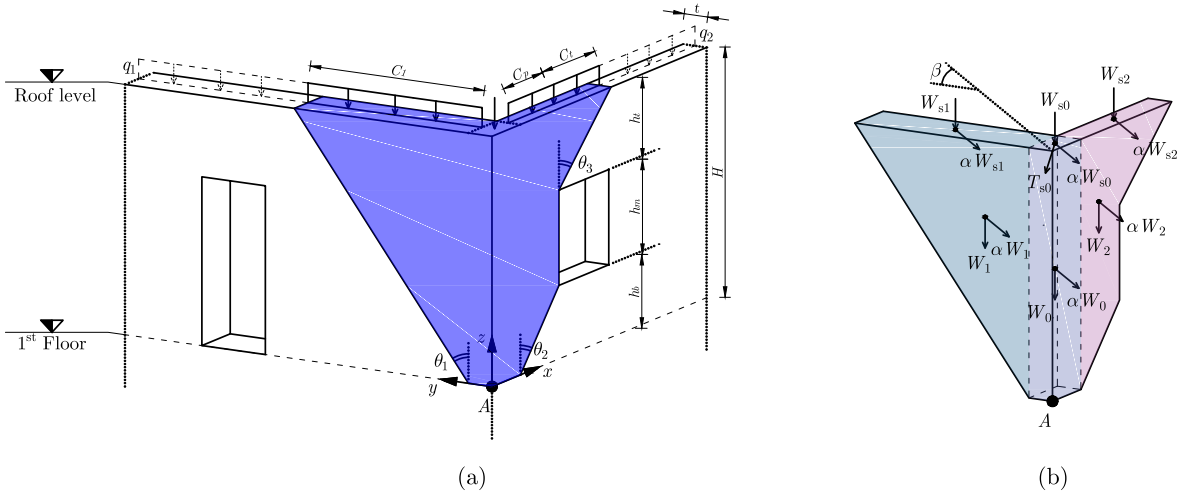

Fig. 12. 3D schematic view of the macro-block involved in the local failure (a) and loads considered in the linear kinematic analysis (b).

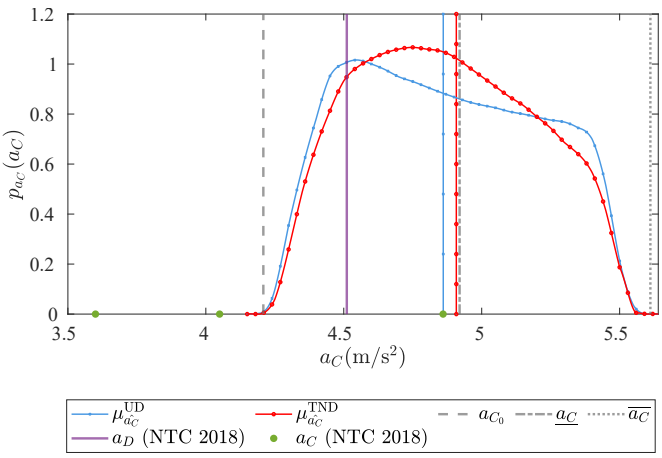

Fig. 14. Corner overturning failure mechanism in the primary school in Visso: LB, UB and PDFs of the acceleration capacity a_C. The additional vertical lines represent the central value of the acceleration capacity a_{Cm} (dashed line) and the mean values μ_{a_C} of the two PDFs (lines with markers). NTC 2018 provisions are represented in terms of acceleration capacity (green dots) and demand (purple line). (For interpretation of the references to colour in this figure legend, the reader is referred to the Web version of this article.)

investigation is applied to a real building. The latter consideration together with the highlighted need to introduce the uncertainties in the models for the out-of-plane local failure mechanisms lead the authors to consider the possibility of incorporating the in-house codes developed for the examined cases in design codes used by engineers in practical applications.

6. Conclusions

In this work, the effects on seismic capacity evaluation due to the introduction of uncertain parameters in the local out-of-plane mechanisms modeling have been investigated. In particular, two commonly observed local failure mechanisms, namely the vertical bending mechanism and the corner overturning mechanism, have been analyzed.

The study of the masonry structure capacity has been based on the upper bound theorem of the limit analysis in terms of the load multiplier parameter and in turn the acceleration capacity. Taking into account a more realistic scenario, some uncertain parameters have been introduced. In particular, in the case of the vertical bending mechanism, the masonry-specific weight and position of the cylindrical hinge have been represented as uncertain parameters. In addition, for the corner overturning mechanism, the uncertain parameter related to the inclination of crack lines with respect to the vertical direction has been introduced.

In order to investigate how the uncertain parameters in the modeling of local out-of-plane mechanisms affect the seismic capacity assessment, two different perspectives have been considered in the representation of uncertain parameters involved.

For the first model, the uncertain parameters are treated as random variables with an assigned probability density function and the PTM is applied to determine the response in terms of probability density functions. On the other hand, in the non-probabilistic uncertainty model, the uncertain parameters are defined as uncertain-but-bounded variables defined solely by a lower bound and an upper bound, then the non-probabilistic interval approach has been applied.

The explicit dependence on uncertain parameters of the seismic response in terms of load multiplier α and acceleration capacity a_C allows us to straightforwardly apply the proposed procedures. Therefore, the role of the uncertainties in the two kinematic models considering both the separate and combined influence of each uncertain parameter, has been assessed.

For the investigation of the vertical bending mechanism, the effect of the uncertain parameters, namely the position of the horizontal cylindrical hinge and the specific weight of the masonry, has been considered by hypothesizing that geometrically the deterministic hinge could be formed both at $0.5h$ and $0.75h$. Therefore, by applying the probabilistic and the non-probabilistic methods to the two different expressions of the PVW, different conclusions can be drawn. Specifically, in the case for which it is assumed that the horizontal cylindrical hinge could be formed at $0.5h$, the introduction of the uncertain parameters non-linearly affects the output results. From the carried out analyses, it is evident the probabilistic method is strongly advised for complete analysis. This is because, even if the interval delineated by the lower and upper bounds represents the entirety of the probability density function's significant space, we cannot have significant additional information inside this interval. Moreover, by comparing the acceleration capacity from the NTC 2018 provisions with uncertain domains obtained with both the probabilistic and non-probabilistic analysis, it is possible to appreciate a good agreement. While, in the case for which it is assumed that the horizontal cylindrical hinge could be formed at $0.75h$, the output results are almost symmetrical and the non-probabilistic analysis can be comprehensive. However, safety assessment is not satisfied for the entire uncertain domain. Specifically, both the lower bound and part of the PDF functions of the acceleration capacity provide values lower than the corresponding acceleration demand.

At last, the effect of the uncertainties on the corner overturning mechanism has been investigated. For this mechanism, uncertain parameters such as the position of the horizontal cylindrical hinge, the specific weight of the masonry, and the crack line inclination have been identified. From the numerical investigations, it is possible to draw that if the effect of uncertain parameters is separately, namely one parameter at a time is considered, then the pieces of information obtained by the interval analysis could be adequate. However, for an extensive study of the combined effects of the uncertain parameters, the application of the probabilistic method is recommended for a fully uncertain analysis. In addition, in the comparison of NTC 2018 provisions in terms of acceleration capacity, the safety assessment is not always satisfied, especially in the case of acceleration capacities corresponding to lower values of load multiplier.

The numerical investigations highlight that in order to compute a reliable estimate of the seismic acceleration capacity, the introduction of uncertain parameters in the modeling of local out-of-plane mechanisms is recommended. Moreover, the comparison of the results from the two different modeling approaches of the uncertain parameters confirms the main results the authors obtained in (Laudani and Santoro, 2022). Namely, the lower and upper bounds estimated by the interval procedures compared with the probability density function, obtained through the application of the PTM, define the integration extremes of the probability density function so as to ensure that the density area has a unitary value.

The findings of this investigation aid the engineer in knowing both the effect of the introduction of uncertain parameters as well as the effect of their modeling, on the masonry structure capacity. In particular, the application of the proposed investigation to a real building that has developed a corner overturning failure mechanism after the 2016–2017 Central Italy earthquake sequence validated that an extensive study of the combined effects of the uncertain parameters is highly recommended.

CRediT authorship contribution statement

Matteo Mazzeo: Conceptualization, Formal analysis, Software, Validation, Writing – original draft, Writing – review & editing. **Rossella Laudani:** Conceptualization, Methodology, Software, Validation, Writing – original draft, Writing – review & editing. **Roberta Santoro:** Conceptualization, Formal analysis, Methodology, Supervision, Validation, Writing – original draft, Writing – review & editing.

Declaration of competing interest

The authors declare that they have no known competing financial interests or personal relationships that could have appeared to influence the work reported in this paper.

Data availability

No data was used for the research described in the article.

References

Argiento, L.U., Maione, A., Giresini, L., et al., 2019. The corner failure in a masonry building damaged by the 2016-2017 central Italy earthquake sequence. In: Proceedings of COMPDYN 2019 7th ECCOMAS Thematic Conference on Computational Methods in Structural Dynamics and Earthquake Engineering. National Technical University of Athens (NTUA), pp. 633–650.

Casapulla, C., Giresini, L., Argiento, L.U., Maione, A., 2019. Nonlinear static and dynamic analysis of rocking masonry corners using rigid macro-block modeling. Int. J. Struct. Stabil. Dynam. 19 (11), 1950137.

Casapulla, C., Argiento, L.U., Maione, A., Speranza, E., 2021. Upgraded formulations for the onset of local mechanisms in multi-storey masonry buildings using limit analysis. Structures 31, 380–394. Elsevier.

Chácara, C., Lourengo, P., Pantò, B., Cannizzaro, F., Caliò, I., 2016. Parametric numerical studies on the dynamic response of unreinforced masonry structures. In: Structural Analysis of Historical Constructions: Anamnesis, Diagnosis, Therapy, Controls. CRC Press, pp. 239–245.

Chácara, C., Cannizzaro, F., Pantò, B., Caliò, I., Lourenço, P.B., 2018. Assessment of the dynamic response of unreinforced masonry structures using a macroelement modeling approach. Earthq. Eng. Struct. Dynam. 47 (12), 2426–2446.

de Felice, G., De Santis, S., Lourenço, P.B., Mendes, N., 2017. Methods and challenges for the seismic assessment of historic masonry structures. Int. J. Architect. Herit. 11 (1), 143–160.

Decreto 17 gennaio 2018: Aggiornamento delle norme tecniche per le costruzioni, 2018. Ministry of Infrastructure and Transport.

Elishakoff, I., Ohsaki, M., 2010. Optimization and Anti-optimization of Structures under Uncertainty. World Scientific.

Falsone, G., Laudani, R., 2020. Closed-form solutions of redundantly constrained stochastic frames. Probabilist. Eng. Mech. 61, 103084.

Giresini, L., Solarino, F., Paganelli, O., Oliveira, D.V., Froli, M., 2019. One-sided rocking analysis of corner mechanisms in masonry structures: influence of geometry, energy dissipation, boundary conditions. Soil Dynam. Earthq. Eng. 123, 357–370.

Giresini, L., Stochino, F., Sassu, M., 2021. Economic vs environmental isocost and isoperformance curves for the seismic and energy improvement of buildings considering life cycle assessment. Eng. Struct. 233, 111923.

Gooch, L.J., Masia, M.J., Stewart, M.G., 2021. Application of stochastic numerical analyses in the assessment of spatially variable unreinforced masonry walls subjected to in-plane shear loading. Eng. Struct. 235, 112095.

Heyman, J., 1966. The stone skeleton. Int. J. Solid Struct. 2 (2), 249–279.

Laudani, R., Falsone, G., 2021. Use of the probability transformation method in some random mechanic problems. ASCE-ASME Journal of Risk and Uncertainty in Engineering Systems, Part A: Civil Engineering 7 (1), 04020054.

Laudani, R., Santoro, R., 2022. An extensive comparative analysis on multi-cracked beams with uncertain damage. Int. J. Mech. Sci. 233, 107594.

Li, J., Chen, J., 2009. Stochastic Dynamics of Structures. John Wiley & Sons.

Lourenço, P.B., Mendes, N., Ramos, L.F., Oliveira, D.V., 2011. Analysis of masonry structures without box behavior. Int. J. Architect. Herit. 5 (4–5), 369–382.

Mendes, N., Lourenço, P.B., 2014. Sensitivity analysis of the seismic performance of existing masonry buildings. Eng. Struct. 80, 137–146.

Moore, R.E., Yang, C., 1996. Interval Analysis. Prentice-Hall, Englewood Cliffs, NJ.

Muscolino, G., Sofi, A., 2012. Stochastic analysis of structures with uncertain-but-bounded parameters via improved interval analysis. Probabilist. Eng. Mech. 28, 152–163.

Muscolino, G., Sofi, A., Zingales, M., 2013. One-dimensional heterogeneous solids with uncertain elastic modulus in presence of long-range interactions: interval versus stochastic analysis. Comput. Struct. 122, 217–229.

Parisi, F., Augenti, N., 2012. Uncertainty in seismic capacity of masonry buildings. Buildings 2 (3), 218–230.

Pulatsu, B., Gonen, S., Parisi, F., Erdogmus, E., Tuncay, K., Funari, M.F., Lourenço, P.B., 2022. Probabilistic approach to assess urm walls with openings using discrete rigid block analysis (d-rba). J. Build. Eng. 61, 105269.

Saloustros, S., Pelà, L., Contrafatto, F.R., Roca, P., Petromichelakis, I., 2019. Analytical derivation of seismic fragility curves for historical masonry structures based on stochastic analysis of uncertain material parameters. Int. J. Architect. Herit. 13 (7), 1142–1164.

Santoro, R., Failla, G., 2021. An interval framework for uncertain frequency response of multi-cracked beams with application to vibration reduction via tuned mass dampers. Meccanica 56 (4), 923–952.

Santoro, R., Muscolino, G., 2019. Dynamics of beams with uncertain crack depth: stochastic versus interval analysis. Meccanica 54 (9), 1433–1449.

Santoro, R., Muscolino, G., Elishakoff, I., 2015. Optimization and anti-optimization solution of combined parameterized and improved interval analyses for structures with uncertainties. Comput. Struct. 149, 31–42.

Santoro, R., Failla, G., Muscolino, G., 2020. Interval static analysis of multi-cracked beams with uncertain size and position of cracks. Appl. Math. Model. 86, 92–114.

Sofi, A., 2015. Structural response variability under spatially dependent uncertainty: stochastic versus interval model. Probabilist. Eng. Mech. 42, 78–86.

Tomić, I., Vanin, F., Beyer, K., 2021. Uncertainties in the seismic assessment of historical masonry buildings. Appl. Sci. 11 (5), 2280.

Valluzzi, M.R., Da Porto, F., Garbin, E., Panizza, M., 2014. Out-of-plane behaviour of infill masonry panels strengthened with composite materials. Mater. Struct. 47, 2131–2145.

Zhang, Y., Wang, Z., Jiang, L., Skalomenos, K., Zhang, D., 2022. Seismic analysis method of unreinforced masonry structures subjected to mainshock-aftershock sequences. Bull. Earthq. Eng. 20 (5), 2619–2641.